ISIJ International, Vol. 53 (2013), No. 3, pp. 520–526

Residual Stress Analysis in PVD Coated Austempered Ductile Iron

Diego Alejandro COLOMBO,[1,2)]* María Dolores ECHEVERRÍA,[1,2)] Osvaldo Julio MONCADA[1,2)] and Juan Miguel MASSONE[2)]

1) Mechanical Technology Group, School of Engineering – Universidad Nacional de Mar del Plata, Av. J. B. Justo 4302, (B7608FDQ) Mar del Plata, Argentina. 2) Metallurgy Division, INTEMA – CONICET, School of Engineering – Universidad Nacional de Mar del Plata, Av. J. B. Justo 4302, (B7608FDQ) Mar del Plata, Argentina.

(*Received on August 28, 2012; accepted on November 6, 2012*)

The aim of this work is to study residual stresses (RS) in PVD TiN and CrN coated ADI substrates with different nodule counts, austempering temperatures and surface finishing methods (grinding and polishing). Coatings were applied by arc ion plating using an industrial reactor and different sets of processing parameters. Residual stress measurements were performed by x-ray diffraction using the $\sin^2\psi$ method along two principal axes on the samples surface (parallel and perpendicular to the substrate abrasion direction). The film thickness, hardness and adhesion of each coated sample were also evaluated.

The results obtained indicate that RS in TiN and CrN coated samples are compressive irrespective of the different substrates, surface finishing methods and processing parameters utilized. The parallel and perpendicular RS do not vary significantly, indicating a rotationally symmetric biaxial stress state. The RS of the coated samples are not influenced by the different substrate characteristics regarding microstructure, hardness and surface roughness. The microhardness and RS of TiN and CrN coated samples increase with film thickness. The increase in substrate temperature together with the decrease in the values of BIAS voltage, arc current and chamber pressure lead to microhardness and RS reduction. Grinding produces surface hardening and reduction of the compressive RS in the substrates, but causes no variations in the RS of the TiN and CrN coated samples. The adhesion strength quality of TiN and CrN coatings to ADI substrates can be related to indices ranging from HF1 to HF2.

KEY WORDS: austempered ductile iron; TiN; CrN; PVD processing parameters; residual stresses; grinding.

1. Introduction

Austempered ductile iron (ADI) is increasingly being used as an application material for the manufacturing of mechanical components due to its wide range of mechanical properties.[1–3)] In applications where components require high wear resistance and must be frequently replaced, surface treated ADI emerges as an advantageous alternative to very high-cost high-strength alloy steels, commonly used in these days. However, any surface treatment involving ADI exposure to high temperature during long periods may cause changes in the ausferritic microstructure and negatively affect the mechanical behavior of the material.[4)]

In the last decade, significant advances have been made in the application of PVD coatings of different materials on ADI substrates. Several authors have accounted for improvements in high cycle fatigue resistance, corrosion resistance and hardness.[5–8)] More recent studies have reported that duplex coatings (electroless nickel and CrTiAlN PVD film) provide better performance against erosive wear than monolithic films and reduce the friction coefficient of ADI.[9)] All these studies applied processing temperatures of up to 300°C and reported no deterioration of ADI microstructure.

On the other hand, the authors of the present work found different sets of industrial-use processing parameters producing PVD TiN and CrN coatings of acceptable characteristics as far as film thickness, hardness and adhesion are concerned, causing no significant deterioration of ADI microstructure.[10)] Additionally, the analysis of the effects of the substrate characteristics on the coating properties evidenced little influence of the austempering temperature and nodule count.[11)] Studies were performed on manual polished substrates with SiC waterproof paper of different grit sizes.

Grinding is one of the most commonly used processes in the industry for surface finishing of mechanical components. The abrasive cutting of grinding produces, depending on the workpiece material in question, wheel characteristics and grinding conditions (workpiece speed, wheel speed and depth of cut per pass), plastic deformation and high temperatures in the workpiece-wheel contact area. As a result, surface hardening and RS are generated, which may affect the service behavior of the components as well as the properties of the coatings deposited.

Coating deposition is inherently associated to RS generation in the film due to the superimposed effect of two components: intrinsic stresses resulted from the nucleation and growth of the film on the substrate, and thermal stresses generated from cooling after deposition due to differences in

* Corresponding author: E-mail: diegocolombo@fi.mdp.edu.ar
DOI: http://dx.doi.org/10.2355/isijinternational.53.520

the thermal expansion coefficients of the film and substrate.[12)]

Generally speaking, PVD processes result in compressive RS that could range from a few GPa to values above –10 GPa.[13–15)] The residual stress state of a coated sample depends on the substrate characteristics, coating materials and processing parameters.[12,16–19)] Surface roughness could also affect the stress state.[20)] Regarding RS influence on the service behavior of coated systems, data reported in the literature indicate that high compressive RS can improve the wear resistance of these systems,[21–24)] however, higher compressive stresses also increase the possibility of film detachment during system duty in tribological applications.[23,24)]

One of the most common techniques for residual stress measurement in thin films is x-ray diffraction (XRD). The traditional XRD technique is known as the $\sin^2\psi$ method.[25)] In this approach, a specific diffraction plane is selected and the interplanar spacing is measured from a sample scan at different specimen tilt angles (ψ), the angle between the diffraction plane normal and the specimen surface normal. Afterwards the residual strain can be derived from the slope of a linear plot between the fractional change of the plane spacing (*i.e.*, strain) and $\sin^2\psi$. In most cases a bi-axial stress model is then used to convert the strain measured into stress.

To the best of the authors' knowledge, there is no information available regarding RS generated in PVD coated ADI substrates, nor about the effects of the substrate surface characteristics due to an industrial-use grinding process on coating properties. On this basis, the aim of this work is to study RS in PVD TiN and CrN coated ADI substrates with different nodule counts, austempering temperatures and surface finishing methods (grinding and polishing). Coatings were applied by arc ion plating using an industrial reactor and different sets of processing parameters. The film thickness, hardness and adhesion of each coated sample were also assessed.

2. Experimental Procedures

2.1. Substrate Material and Samples Preparation

The material utilized in this work was ductile iron produced in a 55 kg middle-frequency induction furnace (3 KHz). The melt was conventionally nodulized and inoculated.[11)] Several 4 and 6 mm thick plates, together with 13 mm Y-blocks, were cast in sand moulds to obtain different nodule counts.

The chemical composition of the material (wt.%), analyzed by optical emission spectrometry, was: C = 3.4; Si = 2.7; Mn = 0.21; S = 0.008; P = 0.027; Mg = 0.033 and Fe balanced. The carbon equivalent was eutectic (CE = 4.3). Based on comparisons with charts, nodularity exceeded 90% in all casting thicknesses.

The plates and Y-blocks were cut and machined by mechanical shaping in order to obtain prismatic samples of approximately 30×30×4 mm. Low-energy cutting conditions were applied to minimize RS generation.

Later, samples were subjected to austempering heat treatments, which consisted in austenitizing at 910°C for 120 min, austempering in a salt bath at temperatures of 280°C and 360°C for 90 min, and subsequent air cooling to room temperature. The samples austempered at 280°C and 360°C were identified as ADI280 and ADI360, respectively.

2.2. Samples Surface Finishing

The heat treated samples were subjected to different surface finishing methods for comparative purposes: an industrial-use grinding process and a laboratory-use polishing process.

Conventional surface grinding was carried out on a horizontal-spindle (peripheral) surface grinder using typical industrial-use cutting conditions. Three roughing passes and one finishing pass were performed on each sample. The finishing pass aims to generate low surface roughness. A vitrified wheel with SiC abrasive grains, identified as IC36/46I/J5V9, was employed. A 5% aqueous solution of Dromus B soluble oil was used as cooling fluid.

On the other hand, a manual polishing using 220 and 1 000 grit sizes SiC waterproof paper was performed in order to obtain different surface roughnesses.

2.3. PVD Coating Process

CrN and TiN coatings were applied by arc ion plating (AIP) in an industrial reactor, using different sets of processing parameters. Prior to deposition, the samples were thoroughly degreased, ultrasonically cleaned, rinsed with alcohol and dried with warm air. Inside the deposition chamber, the samples were cleaned once again by bombardments with energetic ions. **Tables 1** and **2** list the process parameters used to deposit TiN and CrN, respectively.

The authors of the present work reported previously that substrates temperatures close to 300°C with deposition times of up to 240 min did not promote noticeable changes in substrates microstructure, while those performed at temperatures of 400°C and above, as in process B, produced a clear deterioration of the ausferritic microstructure even for short deposition times.[10)] However, the analysis of process B provides elements of interest to the present study.

2.4. Substrates and Coatings Characterization

The values of the average nodule count corresponding to each casting thickness were determined by optical micros-

Table 1. Deposition parameters of TiN coatings.

Process	A	B	C	D	E
Substrate-target distance [mm]	350/200	200	200	200	200
Substrate BIAS voltage [V]	–150	–100	–250	–175	–250
Arc current [A]	60	60	65	60	65
Chamber pressure [Pa]	1.5	0.7	2	1.5	2
Substrate temperature [°C]	280	450	300	300	300
Deposition time [min]	120	45	120	180	240

Table 2. Deposition parameters of CrN coatings.

Process	F	G
Substrate-target distance [mm]	200	200
Substrate BIAS voltage [V]	–175	–175
Arc current [A]	65	60
Chamber pressure [Pa]	2.8	2
Substrate temperature [°C]	300	300
Deposition time [min]	45	150

Table 3. Nodule count and Vickers hardness of the polished substrates.

Sample	Casting thickness [mm]	Nodule count [nod/mm^2]	Hardness [$HK_{0.015}$]
ADI360	13 (Y–block)	494	369 ± 18
	6 (plate)	593	394 ± 13
	4 (plate)	1 056	417 ± 19
ADI280	13 (Y–block)	494	487 ± 21
	6 (plate)	593	513 ± 12
	4 (plate)	1 056	584 ± 20

copy and digital image processing, taking a 5 μm nodule diameter as threshold value. The Knoop hardness (15 g load) of the substrates was established using a microhardness tester. **Table 3** lists the nodule count and Vickers hardness values of the polished substrates.

The conventional arithmetic average roughness (Ra) of the uncoated and coated samples was analyzed using a stylus profilometer (Taylor Hobson Surtronic 3+) with a 4 mm evaluation length (cut-off, 0.8 mm). The measurements were performed along the perpendicular axis to the substrate abrasion direction. In addition, a statistical study of the coated samples roughness was performed using the height-height correlation function $H(r,t)$.[26]

The height–height correlation function contains at least two important parameters: the lateral correlation length ξ and the roughness exponent α. The lateral correlation length ξ provides a length scale which distinguishes the short-range and long-range behaviors of the rough surface. The roughness exponent α describes the local surface roughness. A larger value of α (> 0.5) corresponds to a smooth short-range surface, while the small value of α (< 0.5) corresponds to a more jagged local surface morphology.[27]

Phase identification and residual stress measurements in substrates and coatings were performed by x-ray diffraction (XRD). A Phillips XPERT-PRO diffractometer was utilized, with Cu Kα radiation (λ = 1.5418 Å) at 40 kV and 40 mA.

XRD patterns for phase identification were recorded in a 2θ range from 30° to 150° in steps of 0.02° and with a counting time of 1 second per step.

Residual stress measurements were conducted using the $\sin^2\psi$ method, with the assumption of a biaxial stress state. High diffraction angles, 2θ > 100°, are recommended in order to maximize the peak shift due to stresses, lower the effects of misalignment, and obtain enough data points for the best d-spacing vs. $\sin^2\psi$ plot possible.

In this study the optimal diffraction peaks for the coatings were TiN and CrN (422). Other diffraction peaks were also examined, but proved less suitable than TiN and CrN (422) did. The 2θ angle ranged from 120° to 132° for TiN and from 125° to 135° for CrN, with a 2θ step of 0.05° and 5 seconds per step. The peak profiles were recorded at ψ tilt angles of 0°; 25.29°; 37.17°; 47.73° and 58.69°, respectively.

The optimal diffraction peak for the polished and ground substrates was Fe-α (222). The 2θ angle ranged from 134° to 140°, with a 2θ step of 0.05° and 5 seconds per step. The peak profiles were recorded at ψ tilt angles of 0°; 26.57°; 39.23°; 50.77° and 63.44°, respectively.

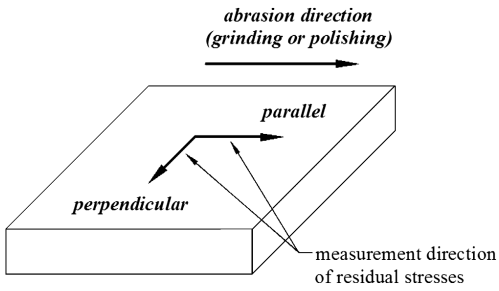

Fig. 1. Measurement directions of RS on the samples surface.

Table 4. X-ray elastic constants of the materials studied.

Material	Lattice plane	S_1 [TPa^{-1}]	½S_2 [TPa^{-1}]	References
TiN	(422)	–0.76	3.61	[25]
CrN	(422)	–1.02	4.75	[26]
Fe-α	(222)	–0.79	4.31	[27]

In order to investigate the anisotropy of the residual stress state, the measurements were carried out along two principal axes on the samples surface (parallel and perpendicular to the substrate abrasion direction). Both directions are shown in **Fig. 1**.

The x-ray elastic constants (XEC's) values used to calculate the stresses in substrates and coatings are reported in **Table 4**.

Coatings thickness was measured on fractured cross sections micrographs, obtained by SEM (JEOL JSM-6460LV).

The Knoop microhardness (15 g load) of the coated samples was determined using a microhardness tester.

Coating adhesion was evaluated using the Rockwell-C adhesion test (150 kg load), using a universal hardness tester.[28]

3. Results and Discussion

3.1. XRD Characterization

Figure 2 illustrates typical x-ray spectrums of uncoated and coated ADI samples. The spectrums of the coated samples not only revealed the coatings main diffraction peaks but also some substrates peaks, since the penetration depth of the X-rays is greater than the film thickness. Regardless of the different substrates, surface finishing methods and processing parameters utilized, TiN and CrN coatings yielded a strong (111) and (220) preferred orientation, respectively.

It is known that for a highly textured coating under the symmetric Bragg-Brentano diffraction geometry, high angle peaks might be too weak to be conveniently measured and may not even be found. Fortunately, TiN and CrN (422) peaks provided sufficient intensity for the accurate determination of peak positions and exhibited the lowest dispersion for residual stress measurement. As an example, **Fig. 3** shows a high angle diffraction pattern of a TiN coated sample wherein reflection (422) can be seen.

3.2. Residual Stress State of Coated Samples

3.2.1. Effect of Substrate Characteristics

Table 5 reports the roughness data of the polished ADI

samples coated with TiN (process C) and CrN (process F) for different nodule counts and austempering temperatures. Polishing condition: 1 000 grit size paper. **Tables 6** and **7** compare the film thickness, microhardness, and RS values of the TiN and CrN coated samples.

The Ra values of the uncoated samples increase as nodule count decreases. As the authors of the present work reported previously,[11] this fact can be ascribed to the coarsening of the matrix as nodule count decreases as well as to the partial or complete graphite removal of certain surface nodules during the polishing stage.

The deposition processes alter the surface roughness of the samples, leading to an increase in Ra. As reported previously,[11] this increase can be assigned to the attachment of Ti or Cr droplets to the growing film which are generated on the target surface during arc evaporation. The lateral correlation length and the roughness exponent for all the TiN coated samples are close to 12.5 μm and 0.85, respectively. This values validate the roughness measurement method employed and the Ra values obtained.

The film thickness of TiN and CrN coated samples is close to 2 μm.

The Knoop microhardness of TiN and CrN coated samples increases as nodule count does and as the austempering temperature decreases, following the hardness trend of their respective substrates (see Table 3).

The RS of the coated samples are compressive, close to -5.6 GPa for TiN and to –3.2 GPa for CrN. The RS in the parallel and perpendicular directions do not vary significantly, indicating a rotationally symmetric biaxial stress state. Similar results has been reported by other authors for CrN

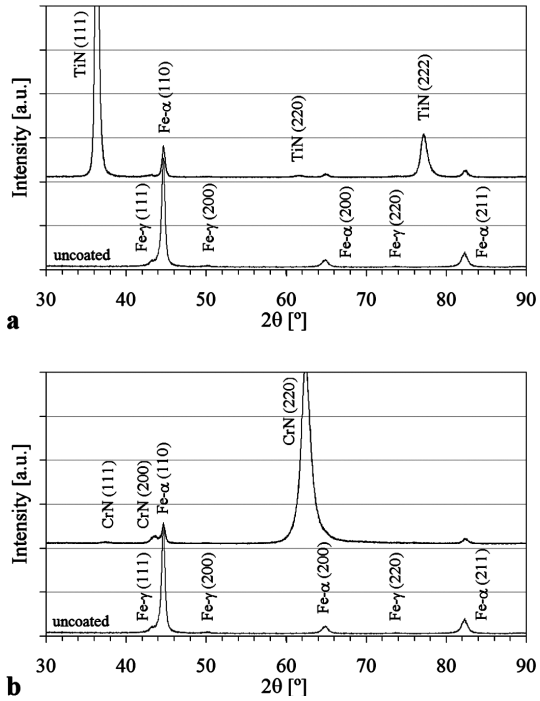

Fig. 2. X-ray spectrums of uncoated and coated samples: (a) TiN – Process D, (b) CrN – Process G.

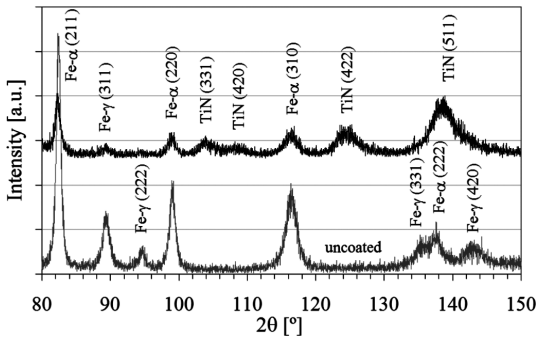

Fig. 3. High angle X-ray spectrum of an uncoated and TiN coated sample.

Table 6. Effect of substrate characteristics on the properties of TiN coated samples.

Sample	Nodule count [nod/mm^2]	Film thickness [μm]	Hardness [$HK_{0.015}$]	Parallel RS [GPa]	Perpendicular RS [GPa]
ADI360	494	1.81 ± 0.13	1 710 ± 36	–5.63 ± 0.11	–5.57 ± 0.12
	593	1.74 ± 0.12	1 785 ± 36	–5.54 ± 0.09	–5.59 ± 0.14
	1 056	2.01 ± 0.13	1 865 ± 49	–5.60 ± 0.12	–5.56 ± 0.14
ADI280	494	2.02 ± 0.13	1 870 ± 32	–5.61 ± 0.10	–5.56 ± 0.13
	593	1.92 ± 0.11	1 951 ± 36	–5.52 ± 0.13	–5.58 ± 0.09
	1 056	1.89 ± 0.15	2 215 ± 47	–5.64 ± 0.12	–5.60 ± 0.10

Table 7. Effect of substrate characteristics on the properties of CrN coated samples.

Sample	Nodule count [nod/mm^2]	Film thickness [μm]	Hardness [$HK_{0.015}$]	Parallel RS [GPa]	Perpendicular RS [GPa]
ADI360	494	2.03 ± 0.19	1 241 ± 35	–3.22 ± 0.13	–3.17 ± 0.12
	593	1.98 ± 0.23	1 296 ± 48	–3.15 ± 0.11	–3.20 ± 0.09
	1 056	2.08 ± 0.29	1 425 ± 33	–3.19± 0.09	–3.17± 0.07
ADI280	494	1.99 ± 0.22	1 413 ± 39	–3.18 ± 0.11	–3.17 ± 0.08
	593	1.89 ± 0.20	1 472 ± 34	–3.13 ± 0.12	–3.16 ± 0.10
	1 056	1.96 ± 0.25	1 561 ± 32	–3.21 ± 0.09	–3.18 ± 0.11

Table 5. Effect of substrate characteristics on the roughness of the uncoated and coated samples.

Sample	Nodule count [nod/mm^2]	Ra [μm]	TiN			CrN
			Ra [μm]	ξ [μm]	α	Ra [μm]
ADI360	494	0.177 ± 0.016	0.210 ± 0.014	12.15 ± 0.66	0.89 ± 0.01	0.264 ± 0.027
	593	0.099 ± 0.010	0.139 ± 0.007	12.87 ± 0.94	0.83 ± 0.01	0.151 ± 0.013
	1 056	0.060 ± 0.011	0.125 ± 0.011	12.74 ± 0.93	0.85 ± 0.01	0.129 ± 0.010
ADI280	494	0.193 ± 0.014	0.271 ± 0.011	12.05 ± 0.72	0.90 ± 0.02	0.231 ± 0.012
	593	0.113 ± 0.010	0.160 ± 0.010	12.16 ± 0.55	0.84 ± 0.01	0.139 ± 0.008
	1 056	0.064 ± 0.011	0.134 ± 0.010	12.64 ± 0.99	0.82 ± 0.02	0.124 ± 0.010

coatings deposited by the same process (ion plating) on steel substrates.[29)]

The different substrate characteristics regarding microstructure, hardness and surface roughness generated by austempering temperature and nodule count variations do not affect the RS values of the coated samples.

The evaluation of the substrate characteristics effect on the RS of the coated samples can be completed with the analysis of their two components: the intrinsic and thermal stresses. The latter can be calculated with the following equation:[30)]

$$\sigma_{th} = \frac{E_f}{1-\upsilon_f}\Delta\lambda\Delta T \ ,$$

where E_f and υ_f are the elastic modulus and the Poisson's ratio of the film, $\Delta\lambda$ is the difference between the expansion coefficients of the film and the substrate, and ΔT is the temperature drop from the deposition temperature to room temperature. **Table 8** lists the elastic and thermal properties of the materials studied in the present work.

The thermal stresses of the different substrates vary from –0.55 to –0.62 GPa for TiN and from –0.69 to –0.74 GPa for CrN. These values are considerably lower than the RS measured. Therefore, the intrinsic stresses generated during film growth on the substrate turned out to be the main component of the RS. Besides, intrinsic stresses are not influenced by the different substrate characteristics.

3.2.2. Effect of Coating Material and PVD Processing Parameters

Table 9 reports the film thickness, microhardness and RS values of the polished ADI samples coated with TiN and CrN for different deposition conditions.

It can be observed that the different deposition conditions promoted a wide range of film thicknesses and hardnesses.

The RS of the coated samples are compressive and cover a range of –4.09 to –6.10 GPa for TiN and of –3.17 to –3.34 for CrN. The RS in the parallel and perpendicular directions do not vary significantly. The values obtained fall within the range reported in the literature for TiN and CrN coatings deposited by PVD techniques on different substrates.[29,31–34)] The RS of the CrN coated samples are significantly lower than those of the TiN coated samples. This fact can be attributed to the lower difference between the lattice parameters of ADI substrates and CrN coatings.

It can also be noticed that the increase in film thickness leads to an increase in microhardness and RS of the coated samples. This behavior has been reported by other authors for TiAlN coatings with film thicknesses similar to those used in this work and deposited by the same process (ion plating) on stainless steel substrates.[35)] RS increase with film thickness is ascribed to the continuous bombardment of the growing film with highly energetic ions, which enhances lattice dilatation and the development of compressive stresses in the film.

In films of similar thickness (processes B and C), a high substrate temperature combined with low values of BIAS voltage, arc current and chamber pressure lead to a reduction of microhardness and RS. In previous works by other authors about RS in TiN, TiAlN and DLC films deposited by various PVD techniques on substrates of different materials, similar results have been reported. It was found that as substrate temperature increases,[36)] and BIAS voltage and arc current decrease,[16,35,37,38)] so does RS.

The adhesion strength quality of TiN and CrN coatings to the polished substrates can be related to indices ranging from HF1 to HF2. Adhesion was affected neither by the different deposition conditions nor by the different substrate characteristics generated by the austempering temperature and nodule count variations. **Figure 4** depicts the imprints resulting from the Rockwell-C adhesion test.

3.2.3. Effect of Substrate Grinding

Table 10 provides the roughness data of the ground and polished ADI samples coated with TiN (process D) and CrN (process G). Polishing condition: 220 grit size paper. **Table 11** compares the film thickness, microhardness, and RS values of the TiN and CrN coated samples.

The Ra values of the substrates are close to 0.19 μm for the different surface finishing methods employed, meanwhile the Ra values of the TiN and CrN coated samples are close to 0.23 μm. The lateral correlation length and the roughness exponent for all the samples are close to 8.6 μm and 0.87, respectively. This suggests that the dynamics of roughness evolution is quite similar during the deposition of the different coatings.[39)]

The film thickness of TiN and CrN coated samples is close to 2.4 μm for the different surface finishing methods employed.

The Knoop microhardness of TiN and CrN coated samples is higher for ground substrates due to the surface hardening producing the abrasive cutting.

The RS of the substrates are compressive and vary with the surface finishing method employed. The RS values of the polished substrates are –0.95 and –0.71 GPa in the parallel and perpendicular directions, respectively. These values are consistent with data reported in a previous work, which explored the effect of the austempering heat treatment on the RS of ductile iron plates.[40)] Consequently, it can be

Table 8. Elastic and thermal properties of the materials studied.

Material	E [GPa]	υ	α [°C^{-1}]	References
ADI	–	–	13.8/14.3e^{-6}	30)
TiN	330	0.25	9.4e^{-6}	11,31)
CrN	245	0.23	6e^{-6}	32,33)

Table 9. Effect of different deposition conditions on the properties of the coated samples.

Process	Film thickness [μm]	Microhardness [$HK_{0.015}$]	Parallel RS [GPa]	Perpendicular RS [GPa]
A – TiN	0.33 ± 0.03	797 ± 65	–4.92 ± 0.11	–4.86 ± 0.10
	1.05 ± 0.10	1 019 ± 69	–5.36 ± 0.10	–5.31 ± 0.14
B – TiN	2.07 ± 0.14	1 307 ± 71	–4.09 ± 0.09	–4.07 ± 0.13
C – TiN	2.02 ± 0.13	1 870 ± 32	–5.61 ± 0.10	–5.56 ± 0.13
D – TiN	2.37 ± 0.46	2 372 ± 104	–5.95 ± 0.14	–5.86 ± 0.09
E – TiN	3.93 ± 0.21	2 838 ± 131	–6.05 ± 0.13	–6.10 ± 0.11
F – CrN	1.99 ± 0.22	1 413 ± 39	–3.18 ± 0.11	–3.17 ± 0.08
G – CrN	2.39 ± 0.31	1 529 ± 90	–3.34 ± 0.10	–3.29 ± 0.10

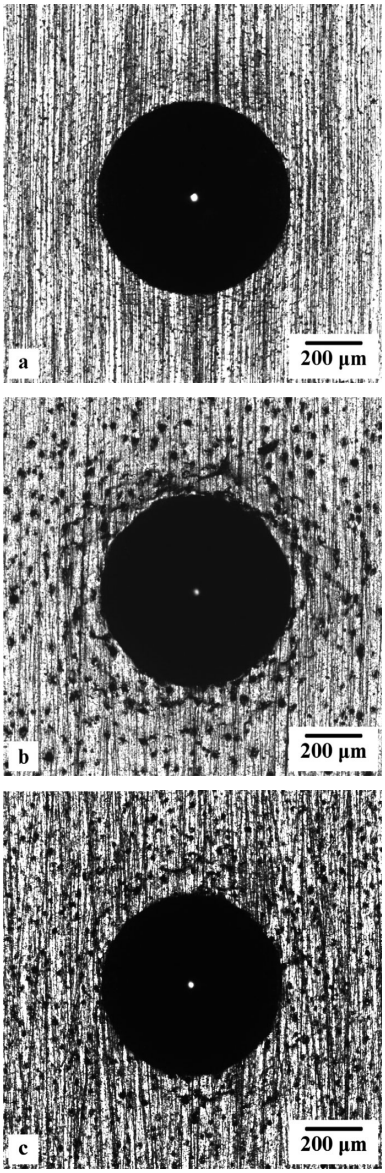

Fig. 4. Imprints on polished samples after Rockwell-C adhesion test: (a) TiN – process A, (b) TiN – process D, (c) CrN – process G.

Table 10. Effect of substrate grinding on the roughness of the uncoated and coated samples.

Sample	Surface finishing method	Ra [μm]	ξ [μm]	α
ADI	Polished	0.192 ± 0.025	–	–
	Ground	0.191 ± 0.028	–	–
ADI-CrN	Polished	0.229 ± 0.029	8.66 ± 0.90	0.87 ± 0.01
	Ground	0.226 ± 0.020	8.54 ± 0.56	0.87 ± 0.01
ADI-TiN	Polished	0.232 ± 0.021	8.55 ± 0.94	0.88 ± 0.01
	Ground	0.231 ± 0.018	8.89 ± 0.85	0.86 ± 0.01

asserted that polishing does not produce significant effects on RS. On the other hand, the cutting conditions employed in the grinding process promote compressive RS reduction. The values of the ground substrates are –0.66 and –0.38 GPa in the parallel and perpendicular directions, respectively.

The RS of the coated samples are not affected by the different surface finishing methods employed. The values are

Table 11. Effect of substrate grinding on the properties of the coated samples.

Sample	Surface finishing method	Film thickness [μm]	Microhardness [$HK_{0.015}$]	Parallel RS [GPa]	Perpendicular RS [GPa]
ADI	Polished	–	375 ± 55	–0.95 ± 0.04	–0.71 ± 0.05
	Ground	–	723 ± 87	–0.66 ± 0.03	–0.38 ± 0.02
ADI-CrN	Polished	2.46 ± 0,36	1 529 ± 90	–3.34 ± 0.10	–3.29 ± 0.10
	Ground	2.38 ± 0,12	1 873 ± 99	–3.27 ± 0.11	–3.31 ± 0.11
ADI-TiN	Polished	2.42 ± 0,60	2 372 ± 104	–5.95 ± 0.14	–5.86 ± 0.09
	Ground	2.51 ± 0,52	2 796 ± 121	–5.94 ± 0.13	–5.87 ± 0.13

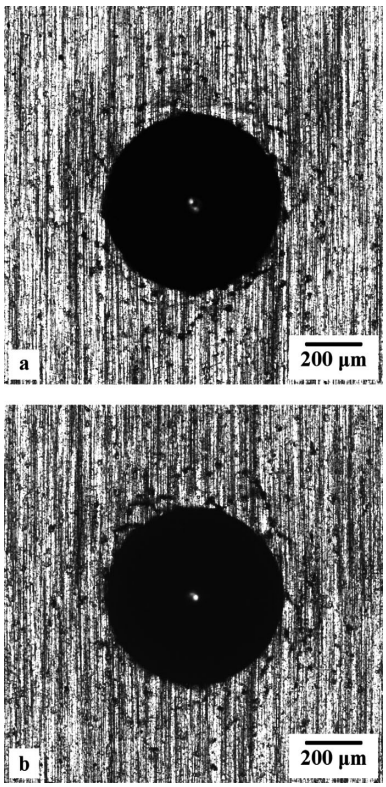

Fig. 5. Imprints on ground samples after Rockwell-C adhesion test: (a) CrN – process G, (b) TiN – process D.

close to –5.9 GPa for TiN and to –3.3 GPa for CrN, independently of the measurement direction. The plastic deformation of the substrates surface layer generated during the grinding process exerts no appreciable influence on the RS of coated samples. It can be seen that the differences in RS values of the coated samples are primarily caused by the coating material.

The adhesion strength quality of TiN and CrN coatings to ground substrates can be related to HF1. As it can be noticed, the abrupt change of properties in the substrate-coating interface with respect to hardness and RS does not exert appreciable influence on adhesion. **Figure 5** illustrates the imprints resulting from the Rockwell-C adhesion test.

It is worth mentioning that the surface characteristics resulting from the different stages of the production process of PVD coated ADI parts, *i.e.*, austempering heat treatment, substrate surface finishing method and PVD coating process, were successfully determined in the present work. Therefore, it can be considered that the data reported herein

may be useful for users and producers of ADI components.

4. Conclusions

TiN and CrN PVD coatings deposited on ADI substrates with different nodule counts and austempering temperatures have a strong preferred orientation, regardless of the surface finishing methods and processing parameters utilized.

RS of TiN and CrN coated samples are compressive. The parallel and perpendicular RS with respect to the substrate abrasion direction do not vary significantly, indicating a rotationally symmetric biaxial stress state.

The different substrate characteristics regarding microstructure, hardness and surface roughness do not affect RS values.

The main variables influencing the microhardness and RS of coated samples are coating material, film thickness and PVD processing parameters.

The RS of the CrN coated samples are significantly lower than those of TiN coated samples.

The different deposition conditions evaluated promote a wide range of film thicknesses. Microhardness and RS of coated samples increase with film thickness.

In films of similar thickness, a high substrate temperature combined with low values of BIAS voltage, arc current and chamber pressure lead to a reduction of the microhardness and compressive RS.

The grinding process produces surface hardening and a reduction of the compressive RS in ADI substrates, however, it causes no variations in the RS of the TiN and CrN coated samples. The adhesion strength quality of the coatings to ground substrates can be related to HF1.

The abrupt change of properties in the substrate-coating interface regarding hardness and RS does not exert appreciable influence on adhesion, although its effect on the behavior of mechanical components subjected to external stresses can be expected to be more significant.

Acknowledgements

The authors wish to thank the company Sudosilo S.A. for its generous collaboration in coatings deposition.

REFERENCES

1) R. A. Martinez, R. E. Boeri and J. A. Sikora: *Trans. Am. Foundry Soc.*, **106** (1998), 27.
2) J. R. Keough: *Eng. Cast. Solut.*, **3** (2001), 42.
3) P. David, J. Massone, R. Boeri and J. Sikora: *ISIJ Int.*, **44** (2004), 1180.
4) J. M. Massone, R. E. Boeri and J. A. Sikora: *Int. J. Cast Met. Res.*, **9** (1996), 79.
5) H. P. Feng, S. C. Lee, C. H. Hsu and J. M. Ho: *Mater. Chem. Phys.*, **59** (1999), 154.
6) C.-H. Hsu, J.-K. Lu and R.-J. Tsai: *Mater. Sci. Eng. A*, **398** (2005), 282.
7) C.-H. Hsu, M.-L. Chen and K.-L. Lai: *Mater. Sci. Eng. A*, **421** (2006), 182.
8) C.-H. Hsu, C.-Y. Lee, K.-L. Chen and J.-H. Lu: *Thin Solid Films*, **517** (2009), 5248.
9) C.-H. Hsu, K.-L. Chen and K.-C. Lu: *Thin Solid Films*, **519** (2011), 4855.
10) D. A. Colombo, M. D. Echeverría, O. J. Moncada and J. M. Massone: *ISIJ Int.*, **52** (2012), 121.
11) D. A. Colombo, M. D. Echeverría, O. J. Moncada and J. M. Massone: *ISIJ Int.*, **51** (2011), 448.
12) K. Holmberg, H. Ronkainen, A. Laukkanen, K. Wallin, S. Hogmark, S. Jacobson, U. Wiklund, R. M. Souza and P. Ståhle: *Wear*, **267** (2009), 2142.
13) H. Oettel, R. Wiedemann and S. Preißler: *Surf. Coat. Technol.*, **74–75, Part 1** (1995), 273.
14) J.-H. Huang, H.-C. Yang, X.-J. Guo and G.-P. Yu: *Surf. Coat. Technol.*, **195** (2005), 204.
15) J.-H. Huang, F.-Y. Ouyang and G.-P. Yu: *Surf. Coat. Technol.*, **201** (2007), 7043.
16) C. A. Carrasco, V. Vergara, R. Benavente, N. Mingolo and J. C. Ríos: *Mater. Charact.*, **48** (2002), 81.
17) M. Bielawski and D. Seo: *Surf. Coat. Technol.*, **200** (2005), 1476.
18) C. Sarioglu, U. Demirler, M. K. Kazmanli and M. Urgen: *Surf. Coat. Technol.*, **190** (2005), 238.
19) O. P. Oladijo, A. M. Venter, L. A. Cornish and N. Sacks: *Surf. Coat. Technol.*, **206** (2012), 4725.
20) J. Mougin, G. Lucazeau, A. Galerie and M. Dupeux: *Mater. Sci. Eng. A*, **308** (2001), 118.
21) T. Z. Kattamis, M. Chen, S. Skolianos and B. V. Chambers: *Surf. Coat. Technol.*, **70** (1994), 43.
22) J. Gunnars and A. Alahelisten: *Surf. Coat. Technol.*, **80** (1996), 303.
23) S. J. Bull: *Wear*, **233–235** (1999), 412.
24) R. C. Cozza, D. K. Tanaka and R. M. Souza: *Surf. Coat. Technol.*, **201** (2006), 4242.
25) U. Welzel, J. Ligot, P. Lamparter, A. C. Vermeulen and E. J. Mittemeijer: *J. Appl. Crystallogr.*, **38** (2005), 1.
26) M. Pelliccione and T. M. Lu: Evolution of Thin Film Morphology: Modeling and Simulations, Springer, Berlín, Heidelberg, New York, (2007).
27) H. N. Yang, Y. P. Zhao, G. C. Wang and T. M. Lu: *Phys. Rev. Lett.*, **76** (1996), 3774.
28) W. Heinke, A. Leyland, A. Matthews, G. Berg, C. Friedrich and E. Broszeit: *Thin Solid Films*, **270** (1995), 431.
29) M. Gelfi, G. M. La Vecchia, N. Lecis and S. Troglio: *Surf. Coat. Technol.*, **192** (2005), 263.
30) H. Oettel and R. Wiedemann: *Surf. Coat. Technol.*, **76–77, Part 1** (1995), 265.
31) L. Cunha and M. Andritschky: *Surf. Coat. Technol.*, **111** (1999), 158.
32) T. Matsue, T. Hanabusa, Y. Miki, K. Kusaka and E. Maitani: *Thin Solid Films*, **343–344** (1999), 257.
33) W.-J. Chou, G.-P. Yu and J.-H. Huang: *Surf. Coat. Technol.*, **149** (2002), 7.
34) K. Valleti, C. Rejin and S. V. Joshi: *Mater. Sci. Eng. A*, **545** (2012), 155.
35) S.-S. Zhao, Y. Yang, J.-B. Li, J. Gong and C. Sun: *Surf. Coat. Technol.*, **202** (2008), 5185.
36) T. Matsue, T. Hanabusa and Y. Ikeuchi: *Thin Solid Films*, **281–282** (1996), 344.
37) M. Ahlgren and H. Blomqvist: *Surf. Coat. Technol.*, **200** (2005), 157.
38) K.-W. Weng, S. Han, Y.-C. Chen and D.-Y. Wang: *J. Mater. Process. Technol.*, **203** (2008), 117.
39) D. Raoufi, A. Kiasatpour, H. R. Fallah and A. S. H. Rozatian: *Applied Surface Science*, **253** (2007), 9085.
40) A. D. Sosa, M. D. Echeverría, O. J. Moncada, N. Míngolo and J. A. Sikora: *J. Mater. Process. Technol.*, **209** (2009), 5545.